

Structural stability of Ni-containing half-Heusler compounds

P. Larson and S. D. Mahanti

Department of Physics and Astronomy, Michigan State University, East Lansing, Michigan 48824

M. G. Kanatzidis

Department of Chemistry, Michigan State University, East Lansing, Michigan 48824

(Received 27 January 2000; revised manuscript received 23 June 2000)

Half-Heusler compounds containing Ni of the form $NiMP$, where M is a trivalent (Sc) or tetravalent (Ti, Zr, Hf) ion and P is a pnictide or stannide ion (Sb, Sn), are known to form semiconducting phases for $M = Sc$ and $P = Sb$ as well as when $M = Ti, Zr, Hf$ and $P = Sn$. However, the electronic structure of these compounds depends sensitively on the relative arrangements of the atoms within the unit cell, changing from a narrow-gap semiconductor to a zero-gap semiconductor to a metal, depending on which of the three atoms lies in the octahedrally coordinated pocket of the NaCl substructure formed by the other two atoms. We have carried out extensive calculations of the total energy for these systems using an all-electron, full-potential method within density-functional theory [using both the local-density approximation and the generalized gradient approximation] to clarify some of the conflicts in earlier calculations using pseudopotential and linear muffin-tin orbital-atomic-sphere approximation methods. The minimum-energy configuration for each of these systems occurs when the Ni atom occupies the octahedrally coordinated pocket formed by the other two elements MP . By comparing the energies of the binary compounds arising from different arrangements of the atoms within the unit cell, we find that the stability of the lowest-energy configuration of the ternary system derives from the energy gained from two sources. The largest source is MP forming in the NaCl substructure rather than a diamond substructure, in agreement with the previous pseudopotential calculations of Ogut and Rabe. Also important are the Ni atoms lying in the octahedrally coordinated pockets and bonding with four M and four P nearest-neighbor atoms rather than forming a part of the NaCl substructure itself. The energies of antisite defects have been investigated by studying the supercell $(NiMP)_4$ formed in the simple cubic structure with individual atoms moved from their ideal positions. We find that the idealized half-Heusler structure (formed by three interpenetrating fcc lattices) has the lowest energy (E_0) while structures where Ni atoms move out of a fcc arrangement, but remain within the octahedrally coordinated pockets of MP , have energies of 0.5-eV/unit cell higher than E_0 , while structures with disorder in the MP NaCl substructure have energies about 1.5-eV/unit cell higher than E_0 . Since the MP disorder and not the Ni disorder is seen experimentally at low temperatures, this Ni disorder may be annealed out while the MP disorder is quenched.

I. INTRODUCTION

Compounds formed in the half-Heusler structure have proven to be an important class of materials in recent years. By chemically tuning the constituents, these materials can change from semiconducting (such as $NiZrSn$, which is of great current interest for thermoelectric applications,¹⁻³) to half-metallic Mn compounds, such as $NiMnSb$,⁴ to fully metallic $NbIrSb$ and $CoTiSn$.⁵ Even for a given set of three elements, say Zr, Ni, and Sn, the arrangement of the atoms within the unit cell can strongly affect the electronic structure. It is therefore critical to understand the energetics of structures with different types of atomic arrangements.

There has been some confusion concerning $NiZrSn$ -type half-Heusler compounds regarding the nature of the ordering of the atoms within the unit cell and which ordering gives the lowest energy. Ogut and Rabe³ (OR), using the local density approximation (LDA) and the pseudopotential plane-wave method, have studied the stability of $NiZrSn$ within three possible configurations and correctly identified the configuration of atoms with the lowest energy, the same configuration as seen experimentally.⁶ They, however, concluded that the inclusion of Ni atoms into the octahedrally coordinated pockets of the NaCl-type basis structure $ZrSn$ had energetically very little effect on the stability of the final compound

$NiZrSn$. This would imply that the Ni atoms essentially enter the above pockets as neutral atoms and do not take part in any sort of bonding with the neighboring Zr and Sn atoms. However, subsequent all-electron full-potential linearized augmented plane-wave (LAPW) calculations [using LDA and the generalized gradient approximation (GGA)] of these materials¹ showed that the hybridization of Ni orbitals with the surrounding Zr and Sn orbitals played a significant role in the gap formation, the effect of Ni atoms was not simply to lower the local symmetry of the binary compound leading to additional hybridization between Zr and Sn orbitals forbidden in the absence of Ni, as envisaged by OR. Therefore, the importance of Ni atoms in the energetics of the stability of the different configurations needs to be investigated in detail.

Furthermore, a recent paper by Ishida *et al.*⁷ analyzed the structural stability of a series of half-Heusler compounds (without reference to the results of OR), using the linearized muffin-tin orbital method in the atomic-sphere approximation (LMTO-ASA) method and LDA, and found that the lowest-energy configurations for most members studied were different from those seen experimentally. This puzzling difference has motivated us to look at the structural stability question using the full-potential LAPW method and both LDA and GGA. We have found that the configuration of the

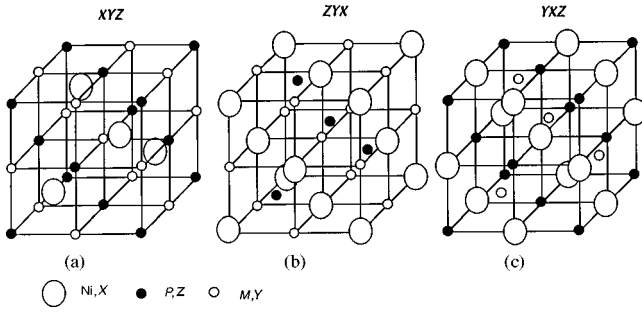


FIG. 1. Crystal structure of half-Heusler compounds in the (a) XYZ, (b) ZYX, and (c) YXZ configurations.

three atoms inside the unit cell which gives the lowest energy agrees with that seen experimentally for all the cases studied.

In order to understand the effects of defects in the half-Heusler structure, a supercell, $(\text{NiMP})_4$, was used for calculations with individual atom's positions different from that of the ideal half-Heusler structure. We have found that certain rearrangements of atoms within this cell are more favorable than others, and we conjecture what effect these antisite defects might have on the electronic structure.

The major point of this paper is to explain the differences between the previous results and ours and to develop a physical understanding of the structural stability of these compounds. In Sec. II we discuss the crystal structure and the method we have used to calculate the total energy of the crystal. In Sec. III we discuss the energetics of the ordered NiMP structures, in Sec. IV we discuss the energetics of antisite defects within the NiMP structure, and in Sec. V we give a summary.

II. CRYSTAL STRUCTURE AND METHOD

Ni-containing half-Heusler compounds, NiMP, with $M = \text{Sc, Ti, Zr, Hf}$ and $P = \text{Sn, Sb}$ form in the MgAgAs structure type (space group: $F4-3m$). The experimental crystal structure⁶ shown in Fig. 1(a) has the NaCl substructure with four Ni atoms within the eight octahedrally coordinated pockets produced by four M and four P atoms. In the full Heusler compound, Ni_2MP , all eight octahedrally coordinated sites are occupied by Ni atoms.

Electronic structure calculations were performed using the self-consistent full-potential LAPW method⁸ within density-functional theory⁹ (DFT) using both LDA of Perdew and Wang¹⁰ and GGA of Perdew, Burke, and Ernzerhof¹¹ for the exchange and correlation potential. The calculations were performed using the WIEN97 package.¹² The values for the atomic radii were chosen in such a manner to minimize the regions between atomic spheres. For each different configuration of the same three elements, the same atomic radii were chosen for each element (Table I). Ishida *et al.*⁷ state that their results were sensitive to the values of the atomic-sphere radii chosen, so extra care has to be taken so that this does not lead to spurious results. Convergence of the self-consistent iterations was obtained with 73 \mathbf{k} points in the reduced Brillouin zone to within 0.0001 Ry, with a cutoff between valence and core states of -6.0 Ry. Scalar relativistic calculations were performed since the spin-orbit inter-

TABLE I. Atomic radii of half-Heusler systems.

System	Atomic radii (a.u.)
NiTiSn	2.33
NiHfSn	2.30
NiZrSn	2.36
NiScSb	2.31
NiScSn	2.37
NiTiSb	2.24

action did not change the energies significantly in these compounds.¹

III. ENERGETICS OF VARIOUS ORDERED STRUCTURES

A. Results for ternary compounds

The possible configurations of the constituent atoms within the unit cell can be written in the same shorthand notation used by Ishida *et al.*⁷ This notation denotes the Ni atom as X, the M atom as Y, and the P atom as Z. The order of X, Y, and Z tells the relative positions of the atoms within the cell. The first letter refers to the atoms within the octahedrally coordinated pockets located at the position $(\frac{1}{4}, \frac{1}{4}, \frac{1}{4})$ while the second refers to the atom at position $(\frac{1}{2}, \frac{1}{2}, \frac{1}{2})$, and the third to the atom at position $(0,0,0)$. Therefore, a configuration designated by XYZ has the Ni atom in the octahedrally coordinated pocket with the M and P atoms forming the NaCl substructure while YXZ exchanges the positions of the Ni and M atoms within the cell⁷ (Fig. 1). These different configurations can also be distinguished by the Greek nomenclatures (α, β, γ) where α refers to the XYZ configuration, β refers to the ZYX configuration, and γ refers to the YXZ configuration, respectively.³

The total LAPW-GGA energies of one system of interest, NiTiSn, for these three different configurations of the constituent atoms in the unit cell as functions of the lattice parameter of the unit cell are given in Fig. 2 (the lowest energy is set to zero). Due to symmetry, interchanging the positions of the atoms composing the NaCl substructure without changing the position of the atom within the octahedrally coordinated pocket gives the same energy within the convergence prescribed by the self-consistent iterations. (Note that elemental site switching for a fraction of the NaCl substructure can affect the total energy and the ternary's semiconducting gap.^{3,13,14}) The configuration which has the lowest energy is XYZ where the Ni atoms lie in the octahedrally coordinated pockets. The energy difference between this lowest-energy structure (XYZ) and the other two structures is about 2 eV/unit cell. The equilibrium lattice parameters for the YXZ and ZYX configurations also differ by about 0.2 Å from that of the XYZ, the XYZ structure being more compact, and there is a small energy difference between the YXZ and ZYX arrangements which is less than 0.1 eV/unit cell. These results are consistent with the earlier calculations for NiZrSn,³ see Fig. 3.

Our LAPW-GGA results for the six different compounds investigated by Ishida *et al.*⁷ are listed in Table II. The first column lists the systems (XYZ) and their experimental lattice parameters (in a.u.), where available. The next three col-

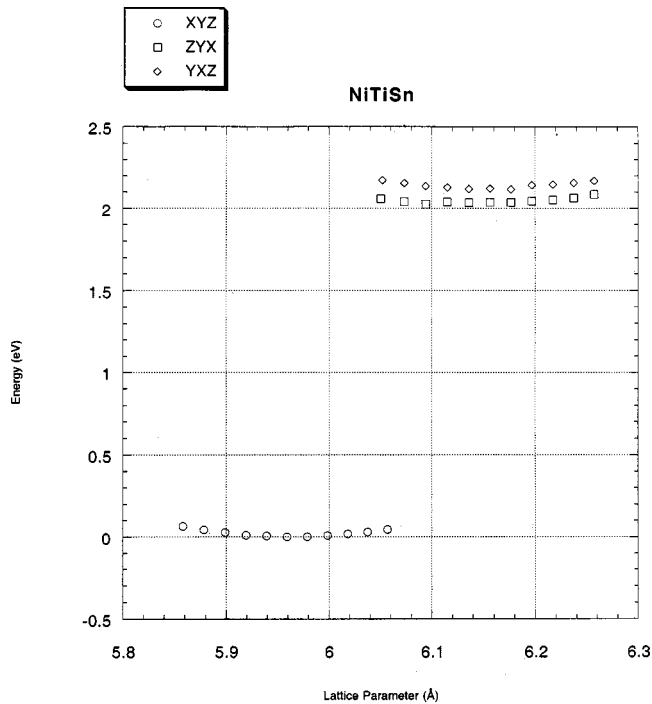


FIG. 2. Total energies as a function of the lattice parameter for the three different configurations of NiTiSn (the lowest energy is set to zero).

umns give the equilibrium lattice parameters of the three types of atomic arrangements while the final three columns give the energy differences (in eV) between different configurations. The configuration for each compound which Ishida *et al.* found to have the lowest energy is italicized. The LAPW-GGA results are dramatically different from

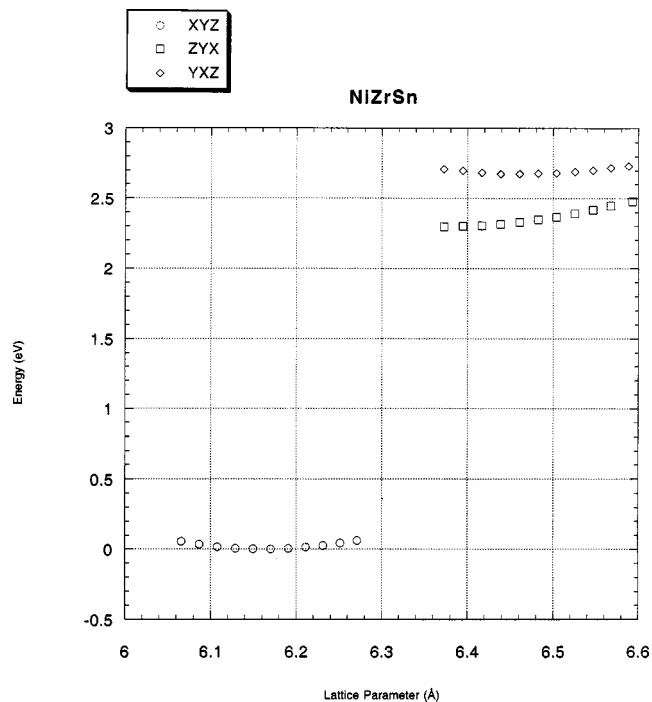


FIG. 3. Total energies as a function of the lattice parameter for the three different configurations of NiZrSn (the lowest energy is set to zero).

those of LMTO-ASA LDA,⁷ but these LAPW-GGA results for NiZrSn agree very well with those for the pseudopotential LDA.³ In order to see whether the differences between LMTO-ASA and LAPW results are due to the difference between LDA and GGA, the energy differences within LAPW were calculated using LDA for NiZrSn. GGA and LDA energy differences are found to be within 1–2%. It should also be noted that the lattice parameters for the lowest-energy configuration (*XYZ*), where Ni atoms occupy the octahedrally coordinated pockets of the NaCl substructure formed out of *YZ*, agree fairly well with the experimental values whereas the configurations with Ni in the NaCl substructure (*YXZ* and *ZYX*) tend to have a larger lattice parameter by 3–6% which are in poor agreement with experiment.

A comparison of the electronic structures of the three different configurations shows that interchanging the position of the atoms within the unit cell has a profound effect. The electronic structures of the NiTiSn system is given in Fig. 4 in the *XYZ* (NiTiSn), *ZYX* (SnTiNi), and *YXZ* (TiNiSn) configurations, respectively. These results agree with the previous calculations⁷ where the lowest-energy configuration, NiTiSn, forms a narrow-gap semiconductor, with the top of the valence band at Γ , and the bottom of the conduction band at X . The SnTiNi structure forms a zero-gap semiconductor where the lowest conduction band along Δ moves down drastically such that its minimum is degenerate with the top of the valence band. In the highest-energy configuration, TiNiSn, a conduction band moves down dramatically near the X point and a valence band goes up near the K point to give a metallic system. The above-mentioned trends for the closure of the gap exist for all the four semiconducting compounds studied (NiTiSn, NiHfSn, NiZrSn, NiScSb). For NiZrSn, the semiconducting *XYZ* configuration changes to a zero-gap semiconductor in the *ZYX* configuration and becomes completely metallic in the *YXZ* configuration (Fig. 5). This is in complete agreement with the earlier pseudopotential calculations of OR.³

It is unclear from the paper of Ishida *et al.*⁷ which lattice constants were used in their calculations. Also, the values of the energy differences between the different configurations were not given and the nature of the electronic states of these half-Heusler compounds in configurations other than *XYZ* were not discussed. In view of our present calculations, their suggestion that these half-Heusler systems can exist in configurations other than *XYZ* it is not very likely. Also it would disagree with several experiments on these materials.⁶

B. Results for binary subsystems with fixed and relaxed lattice parameters

Since we have found that the *XYZ* configuration has the lowest energy for each of the systems studied, it is important to understand which pairs of elements within a particular configuration contributes most to the total stability of the ternary compound. In order to understand the relative energy contributions to the binding energy of pairs of atoms in the unit cell, we follow OR who performed energy calculations of binary subsystems which appear in different ternary configurations. This technique may be crude, but it can give information about which types of bondings are important in

TABLE II. Experimental and calculated equilibrium lattice parameters and total-energy differences for half-Heusler systems (GGA). (For identification of XYZ , ZYX , and YXZ , please see text.)

System	Expt. (XYZ) (a.u.)	XYZ (α) (a.u.)	ZYX (β) (a.u.)	YXZ (γ) (a.u.)	$ZYX - XYZ$ (eV)	$YXZ - XYZ$ (eV)	$YXZ - ZYX$ (eV)
NiTiSn	11.187	11.261	11.516	11.595	2.03	2.12	0.09
NiHfSn	11.463	11.572	11.955	12.150	2.43	2.67	0.24
NiZrSn	11.546	11.607	12.042	12.168	2.30	2.68	0.38
NiScSb	11.442	11.607	11.942	12.107	1.66	2.39	0.74
NiScSn	NA	11.690	12.080	12.121	2.23	2.19	-0.01
NiTiSb	11.187	11.291	11.589	11.663	1.51	1.37	-0.14

the stability of the half-Heusler structure. In order to better understand the energetics of the ternary systems, the lattice parameters were relaxed within LAPW-GGA and LAPW-LDA to find the lowest-energy configuration. We want to understand whether this relaxation of the lattice parameters

has any effect on the energetics of the binary compounds. For example, let us consider the NiZrSn system and the NiZr binary. In the XYZ configuration, NiZr forms a diamond structure whereas in the ZYX configuration NiZr forms a NaCl structure. It is important to understand how the energy

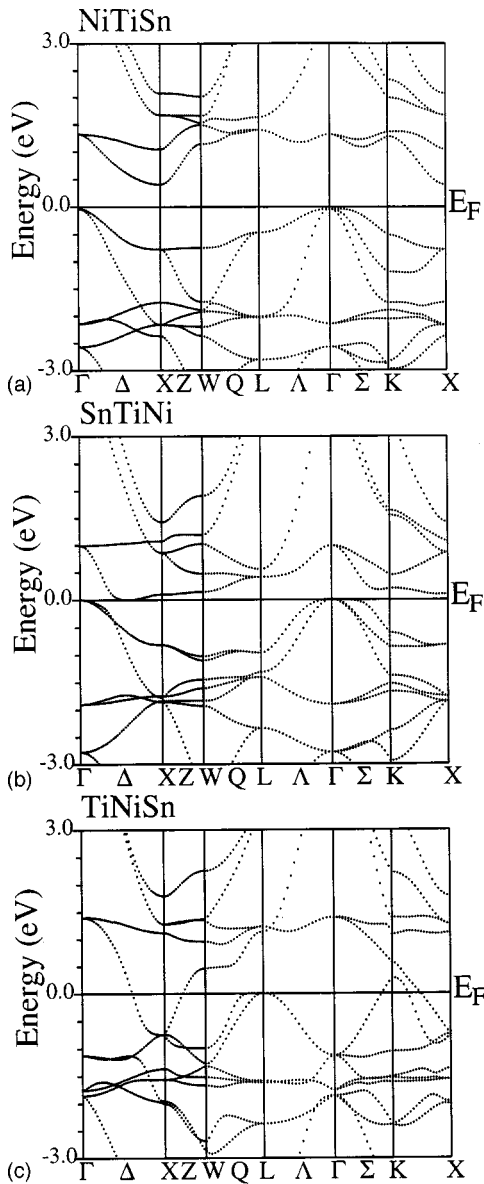


FIG. 4. The electronic structures of the (a) XYZ , (b) ZYX , and (c) YXZ configurations of NiTiSn.

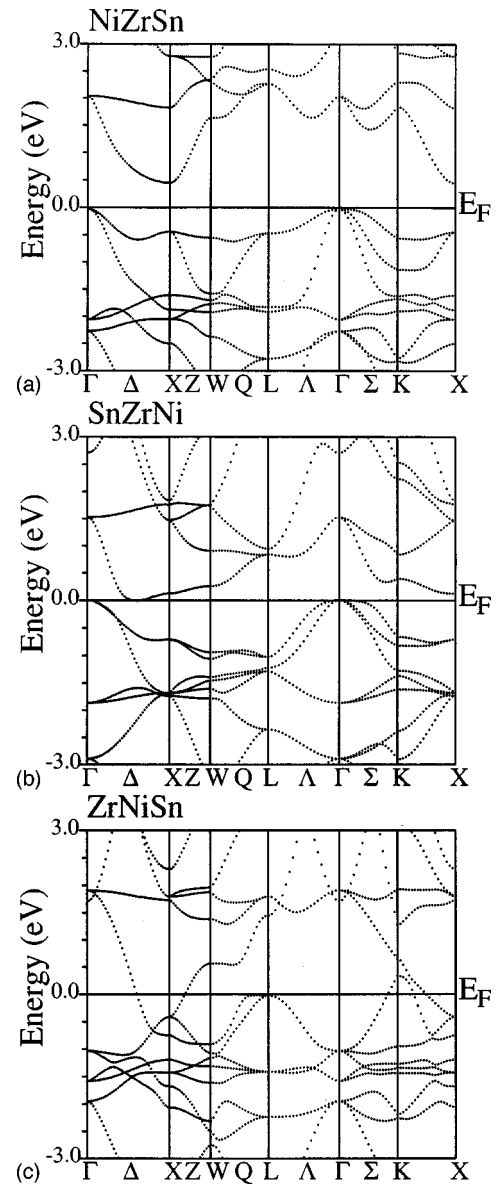


FIG. 5. The electronic structures of the (a) XYZ , (b) ZYX , and (c) YXZ configurations of NiZrSn.

TABLE III. Total-energy differences for NiZrSn and different binary systems with fixed lattice parameters calculated using the pseudopotential within LDA [Ogut and Rabe (Ref. 3)] and using the LAPW within LDA and GGA (present calculation).

NiZrSn	<i>XYZ</i>	<i>ZYX</i>	<i>YXZ</i>	<i>ZYX</i> - <i>XYZ</i>	<i>YXZ</i> - <i>XYZ</i>	<i>YXZ</i> - <i>ZYX</i>
Pseudopotential (LDA) [calculated by Ogut and Rabe (Ref. 3)]						
11.546 a.u.				2.28 eV ^a	2.85 eV ^a	0.57 eV ^a
ZrSn	NaCl	Diamond	Diamond	Diamond-NaCl 2.03 eV	Diamond-NaCl 2.03 eV	Diamond-diamond 0 eV
NiZr	Diamond	NaCl	Diamond	NaCl-diamond 0.26 eV	Diamond-diamond 0 eV	Diamond-NaCl -0.26 eV
NiSn	Diamond	Diamond	NaCl	Diamond-diamond 0 eV	NaCl-Diamond 0.23 eV	NaCl-diamond 0.23 eV
LAPW (LDA)						
11.546 a.u.				2.63 eV	3.29 eV	0.66 eV
ZrSn	NaCl	Diamond	Diamond	Diamond-NaCl 2.03 eV	Diamond-NaCl 2.03 eV	Diamond-diamond 0 eV
NiZr	Diamond	NaCl	Diamond	NaCl-diamond 0.50 eV	Diamond-diamond 0 eV	Diamond-NaCl -0.50 eV
NiSn	Diamond	Diamond	NaCl	Diamond-diamond 0 eV	NaCl-diamond 0.76 eV	NaCl-diamond 0.76 eV
LAPW (GGA)						
11.546 a.u.				2.60 eV	3.25 eV	0.65 eV
ZrSn	NaCl	Diamond	Diamond	Diamond-NaCl 2.33 eV	Diamond-NaCl 2.33 eV	Diamond-diamond 0 eV
NiZr	Diamond	NaCl	Diamond	NaCl-Diamond 0.22 eV	Diamond-diamond 0 eV	Diamond-NaCl -0.22 eV
NiSn	Diamond	Diamond	NaCl	Diamond-diamond 0 eV	NaCl-diamond 0.51 eV	NaCl-diamond 0.51 eV

^aEnergy differences for ternary compounds calculated by OP (Ref. 3) computed at relaxed lattice parameters.

differences associated with the binary compounds change as the lattice of the ternary compound is relaxed.

In the analysis of the binary systems energetics carried out by OR, all energies for the binaries were calculated at the same lattice parameter, but they were compared with the energies of the ternary compounds obtained at different lattice parameters. This appears to be inconsistent because one should allow for lattice relaxation effects in comparing the energies of the binaries also. But before doing that we first discuss the binary energy calculations following exactly the same method of OR, but using the all-electron LAPW method (both within LDA and GGA) to see if there are differences in relative energies that depend on the method of calculation (pseudopotential vs LAPW both using LDA) and the different approximations to the exchange and correlation potential (LDA vs GGA within LAPW). Our results are given in Table III.

The first column of Table III gives the names of the binary systems of interest. The following three columns give the crystal structure of the binary derived from the half-Heusler structure. The last three columns give the energy differences between different configurations. The same lattice parameter, 11.546 a.u., was used in all the calculations. First, it is important to compare the energy differences within LDA comparing pseudopotential and LAPW methods. The difference in energy between the *XYZ* and *ZYX/YXZ* configurations in ZrSn agrees very well with OR's result. On the other hand, the NiZr energy difference is

0.50 eV compared to 0.26 eV found by OR. Similarly, the energy difference between the diamond and NaCl structures of NiSn is found to be 0.76 eV compared to 0.23 eV found by OR. The diamond structure for NiZr has the lowest energy, as does the diamond structure of NiSn and the NaCl structure of SnZr, all of which as found in the ternary *XYZ* configuration of NiZrSn. The energy differences for SnZr in the NaCl and diamond phases are larger than the energy differences found between the diamond and NaCl phases of NiZr or NiSn, but not as large a difference as a factor of 10 found by OR, but more on the order of a factor of 3 or 4. The results from the pseudopotential calculations³ indicate that in the ternary NiZrSn compound, the Ni *d* contribution is inconsequential near the Fermi energy, while a significant Ni *d* state contribution is found just above the Fermi energy in a more accurate LAPW calculation.¹ Finally, a comparison of LDA and the GGA results in LAPW shows that the energy differences for the ternary compounds change very little. The energy difference between the *XYZ* and *ZYX/YXZ* configurations is slightly larger using GGA (by about 0.30 eV/unit cell), but the energy differences between the *XYZ* and *ZYX/YXZ* configurations for NiZr and NiSn are lower than the LDA results (by about 0.25 eV/unit cell). In fact, the pseudopotential-LDA agrees better with LAPW-GGA rather than with LAPW-LDA.

The above binary subsystem energetics calculations were carried out for the same lattice parameter. But we know that the equilibrium lattice parameters can differ by a large

TABLE IV. Relaxed equilibrium lattice parameters and total-energy differences for NiZrSn and different binary subsystems calculated using LAPW within LDA and GGA.

NiZrSn	XYZ	ZYX	YXZ	ZYX-XYZ	YXZ-XYZ	YXZ-ZYX
LAPW (LDA)						
11.546 a.u. ^a	11.429 a.u.	11.735 a.u.	11.928 a.u.	2.50 eV	2.98 eV	0.48 eV
ZrSn	NaCl	Diamond	Diamond	Diamond-NaCl 1.99 eV	Diamond-NaCl 1.89 eV	Diamond-diamond -0.10 eV
NiZr	Diamond	NaCl	Diamond	NaCl-Diamond 1.08 eV	Diamond-diamond 0.72 eV	Diamond-NaCl -0.37 eV
NiSn	Diamond	Diamond	NaCl	Diamond-diamond 0.32 eV	NaCl-diamond 1.49 eV	NaCl-diamond 1.17 eV
LAPW (GGA)						
11.546 a.u.	11.261 a.u.	12.042 a.u.	12.168 a.u.	2.30 eV	2.68 eV	0.38 eV
ZrSn	NaCl	Diamond	Diamond	Diamond-NaCl 1.78 eV	Diamond-NaCl 1.71 eV	Diamond-diamond -0.07 eV
NiZr	Diamond	NaCl	Diamond	NaCl Diamond 1.16 eV	Diamond-diamond 0.68 eV	Diamond-NaCl -0.47 eV
NiSn	Diamond	Diamond	NaCl	Diamond-diamond 0.36 eV	NaCl-diamond 1.30 eV	NaCl-diamond 0.95 eV

^aExperimental value (Ref. 3).

amount depending upon the structure (*XYZ*, *ZYX*, *YXZ*). To get a better understanding of the relative importance of pairs of atoms in the structural stability, we carried out energy calculations for the binary subsystems within both LDA and GGA (Table IV) using the *relaxed* lattice parameters of the ternaries, rather than a *fixed* lattice parameter appropriate for the ternary with the lowest energy. As before, the first column lists the binary compounds while the next three columns give their crystal structure as derived from the half-Heusler structure and the respective equilibrium lattice parameters. The last three columns list the energy differences between the configurations of the binary compounds.

For NiZrSn the energy difference between the *XYZ* and the *ZYX*(*YXZ*) configuration for LDA is 2.50 eV (2.98 eV)/unit cell and for GGA is 2.30 eV (2.68 eV)/unit cell whereas the difference between the energies of the ZrSn substructure originating from the *XYZ* and *ZYX*(*YXZ*) configurations for LDA is 1.99 eV (1.89 eV)/unit cell and for GGA is 1.78 eV (1.71 eV)/unit cell, about three-fourths of the energy gain found in the ternary. The energy difference between the *XYZ* and *ZYX* structures for NiZr is 1.081 eV for LDA and 1.160 eV for GGA, 30–50 % less than that for ZrSn. Similarly, the energy difference between the *XYZ* and *YXZ* structures for NiSn is 1.491 eV for LDA and 1.304 eV for the GGA, each about 25% less than that for ZrSn. Comparing these numbers to those obtained at fixed lattice parameters, it is clear that relaxation has a strong effect on the relative energies of the binary compounds. For example, comparing the NaCl and diamond phases of NiZr and ZrSn, for GGA the NiZr energy difference is only 10% of that for ZrSn using the fixed lattice parameters but becomes 65% that of ZrSn using the relaxed parameters. We have found that the LAPW-LDA and LAPW-GGA energy differences were very similar to the pseudopotential-LDA energy differences when the lattice parameters were fixed. Also, the LAPW-LDA and LAPW-GGA energy differences using the relaxed lattice parameters were very similar. Since the difference in the energies de-

pends most strongly on relaxation or no relaxation of the lattice parameters, either LDA or GGA can be used to compare the energies of different configurations.

The energy gained from ZrSn forming in the NaCl structure is larger than the energy differences when NiSn or NiZr form in the diamond instead of the NaCl structure. Therefore, ZrSn forming the NaCl framework of the ternary has the largest role of any pair of atoms in contributing to the structural stability of the half-Heusler compounds, in agreement with the findings of OR.³ However, upon relaxation, the energy differences between different configurations for NiSn and NiZr are no longer small, and they play a substantial role in having the Ni form in the diamond structure with Zr or Sn. Therefore, although a major factor in the total stability of these ternary half-Heusler compounds is the ZrSn NaCl substructure, there is a significant contribution to this stability from the Ni atoms entering the octahedrally coordinated pockets.

From the arguments presented above, we believe the Ni atoms play an active role in the energy stabilization of these compounds. The position of the Ni atom within NaCl substructure or in the octahedrally coordinated pockets formed by the *MP* NaCl substructure controls whether the system is a narrow-gap semiconductor, a zero-gap semiconductor, or a metal. Comparison of the Ni *d* character overlying the plots of NiTiSn (Fig. 6) shows that the *XYZ* configuration has much more Ni *d* character approximately 2 eV below the Fermi energy while the Ni *d* character becomes more prominent near the Fermi level when Ni is moved to the NaCl substructure. This can be understood by the eightfold bonding within the pocket (to four Zr and four Sn at a distance ~ 2.6 Å) to fourfold bonding (to either four Sn or four Zr at a distance ~ 3.0 Å) when Ni is in the NaCl substructure (Fig. 1). The increased number of bonds stabilizes the structure so that the Ni acts more like a Ni atom.

A few general comments can be made about the results obtained when comparing the energies of the binary and ter-

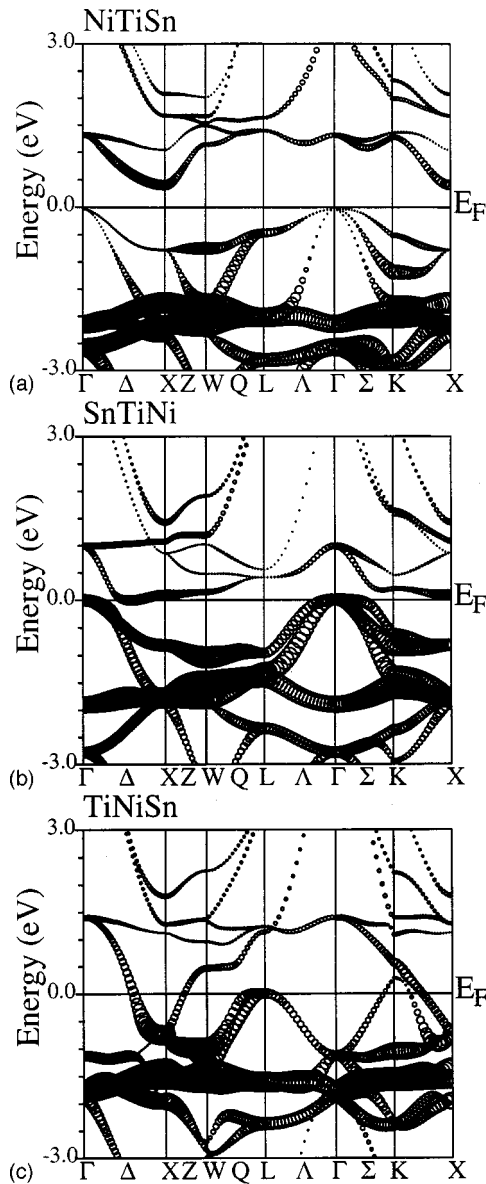


FIG. 6. The electronic structures of the (a) XYZ, (b) ZYX, and (c) YXZ configurations of NiZrSn with the Ni d character at each point printed proportional to the circle at that point.

nary compounds. It should be noted that the ordering of energies of the ZYX and YXZ structures is reversed for the binary compounds compared to the energies of their ternary parent compounds (when the XYZ structure forms a semiconductor). Therefore, the insertion of the third element must play some role in the stabilization of the energy (compare the final column of Table II with that of Table IV). It is also interesting to note that the total energies of metallic NiTiSb and NiScSn for the YXZ and ZYX are reversed with respect to which has the lower energy compared to the ordering of the semiconductors. In the case where the XYZ configuration forms a semiconducting state, the ZYX configuration forms a zero-gap semiconductor having a higher energy whereas the metallic YXZ configuration has the highest energy. Since the XYZ, YXZ, and ZYX configurations are metallic for NiTiSb and NiScSn, a zero-gap semiconductor cannot form to lower the energy of ZYX with respect to the metallic YXZ. However, the XYZ configuration remains the ground

state of NiTiSb and NiScSn, a combination of the stability of the MP substructure and the eightfold versus sixfold coordination of the Ni atom.

IV. ENERGETICS OF POSSIBLE ANTISITE DEFECTS IN THE NiMP STRUCTURE

Electronic structure calculations of NiMP compounds have shown to have a larger gap than has been measured experimentally^{3,13,14} OR performed a series of calculations within the virtual-crystal approximation for $\text{Ni}(\text{Sn}_{1-x}\text{Zr}_x)(\text{Sn}_x\text{Zr}_{1-x})$ for a few values of x lying between $x=0$ and $x=0.5$. They found that the band gap decreased with increasing x to produce a semimetal when $x=0.15$.³ This observation has been given as a possible reason for the smaller value of the experimental gap (~ 0.187 eV) (Ref. 15) compared to the theoretical value of the ordered NiZrSn (~ 0.51 eV).^{13,14}

The above argument for the band-gap reduction is based on x-ray diffraction studies done at low temperatures (< 250 K) which found antisite disorder in the ZrSn NaCl sublattice but no disorder in the Ni sublattice, out of a fcc configuration, after annealing.¹⁶ The temperature range in which these materials are expected to be used for thermoelectric applications is anywhere from 300 to 700 K,⁶ where the structure has not been fully investigated. In fact, a Ni-defect phase was detected before annealing with different lattice parameters a_I and a_{II} which disappear after annealing.¹⁵ Therefore, defects in the Ni sublattice within the MP framework and their effect on the electronic structure need to be investigated.

Here we investigate the energetics of partial disorder of both the Ni and ZrSn sublattices by performing total-energy calculations using the cubic supercell $(\text{NiZrSn})_4$. By changing the positions of the 12 available atoms (four Ni, four Zr, four Sn) within the cell from their ideal half-Heusler positions (eight sites of the NaCl sublattice originally occupied by Zr and Sn atoms and four of the eight octahedrally coordinated sites originally occupied by Ni atoms), one can see which types of disorder are energetically more favorable.

We find that changing the positions of the Sn/Zr atoms with the Ni atoms or other Zr/Sn atoms within the supercell produces a fairly large increase in the energy. Using the same relaxed lattice parameter and atomic radii as in the fcc calculations, the total energies were calculated for the four systems listed in Table V (Fig. 7). As can be seen, switching one Ni and one Zr (Sn) atom increases the energy by a fairly large amount (1.71 eV/fcc unit cell and 1.98 eV/fcc unit cell) while switching one Zr and one Sn atom has a smaller energy increase (1.25 eV/fcc unit cell). This is in agreement with our earlier statements of the stability of the MP NaCl substructure and the greater stability of Ni atoms within the octahedral pockets of MP. In order to understand how the Zr/Sn environment about Ni affects the energy and the band structure, we interchanged one Zr and one Sn atom, first in Zr_4Sn_4 (no Ni atoms) and then in $\text{Ni}_4\text{Zr}_4\text{Sn}_4$. The energy for Zr_4Sn_4 increased by 1.10 eV/fcc unit cell, but increased by 1.25 eV/fcc unit cell for $\text{Ni}_4\text{Zr}_4\text{Sn}_4$. Therefore, the interaction of Ni atoms with the changed Zr/Sn environment increases the energy by only 0.15 eV/fcc unit cell, but the band structures become metallic. From the above analysis, we can conclude that (i) disorder of the ZrSn sublattice has a fairly

TABLE V. Energetics of site-switching on NaCl substructure of NiZrSn supercell (GGA).

System	Energy-energy Ni ₄ Zr ₄ Sn ₄ (eV)	ΔE /fcc unit cell (eV)
Ni ₄ Zr ₄ Sn ₄	0	0
Ni ₄ (Zr ₃ Sn)(Sn ₃ Zr)	4.99	1.25
(Ni ₃ Sn)Zr ₄ (Sn ₃ Ni)	6.82	1.71
(Ni ₃ Zr)(Zr ₃ Ni)Sn ₄	7.93	1.98
Zr ₄ Sn ₄	0	0
(Zr ₃ Sn)(Sn ₃ Zr)	4.39	1.10

high energy cost, but not as high a cost as moving the Ni atoms from the octahedrally coordinated pockets to the NaCl sublattice and (ii) in both cases the system becomes metallic. As mentioned previously, OR found that this system becomes a semimetal for 15% Zr/Sn disorder³ while all of our calculations have at least 25% disorder.

A different scenario for antisite defects in half-Heusler compounds is for the Ni atoms not to arrange in a fcc configuration within the octahedrally coordinated pockets of MP, but rather have antisite defects form between the Ni atoms and the empty sites. In order to investigate this possibility, the total energies of several rearrangements of the Ni sublattice have been calculated, again using the same lattice parameter and atomic radii as for the relaxed fcc unit cell (Table VI). The first configuration is obtained by moving one Ni atom into one of the four empty sites [Fig. 8(a)]; the second configuration is obtained by moving two Ni atoms into empty sites to form an eclipsed arrangement [Fig. 8(b)]; and the third configuration is obtained by moving two Ni atoms into empty sites to form a staggered arrangement [Fig. 8(c)]. The energy increases above the half-Heusler structure of these three configurations are much smaller than those associated with the rearrangements of the NaCl substructure by about a factor of 2 (0.6–0.8 eV/fcc unit cell compared to 1.3–2.0 eV/fcc unit cell). These systems are also metallic, but there are fewer bands crossing the Fermi energy compared to the systems with disorder of the NaCl substructure.

V. SUMMARY AND CONCLUSIONS

In summary, our LAPW-GGA and LAPW-LDA total-energy calculations showed that in all the six compounds with half-Heusler structure that we have studied, the lowest-

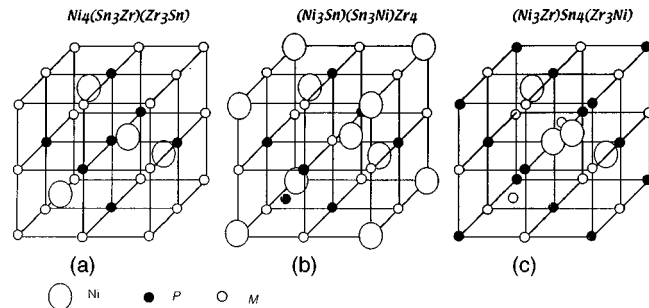


FIG. 7. Crystal structures of the $(\text{NiMP})_4$ supercell for (a) $\text{Ni}_4(\text{Zr}_3\text{Sn})(\text{Sn}_3\text{Zr})$, (b) $(\text{Ni}_3\text{Sn})\text{Zr}_4(\text{Sn}_3\text{Ni})$, and (c) $(\text{Ni}_3\text{Zr})(\text{Zr}_3\text{Ni})\text{Sn}_4$.

TABLE VI. Energetics of site-switching on Ni substructure of NiZrSn supercell (GGA).

System	Energy-energy (Ni ₄ Zr ₄ Sn ₄) (eV)	ΔE /fcc unit cell (eV)
Ni ₄ Zr ₄ Sn ₄	0	0
Ni ₄ Zr ₄ Sn ₄ -8a	2.37	0.59
Ni ₄ Zr ₄ Sn ₄ -8b	2.66	0.67
Ni ₄ Zr ₄ Sn ₄ -8c	3.14	0.78

energy configuration is the one where the Ni atoms occupy the octahedrally coordinated pockets of the NaCl substructure formed by the other two elements. Since the metallic NiScSn and NiTiSb have this XYZ structure as its lowest-energy configuration, the formation of a semiconducting gap is not necessary to explain why this configuration has the lowest energy. The structural stability of these Ni-containing half-Heusler compounds (denoted as NiMP , $M = \text{Sc, Ti, Zr, Hf}$; $P = \text{Sc, Sb}$) arises from two main sources. The first is the higher stability of the binary compound MP in the NaCl substructure over the diamond substructure. The second is the increased stability of the Ni d levels when placed within the pockets to form eight nearest-neighbor bonds rather than six nearest-neighbor bonds when Ni atoms are in the NaCl substructure. The compounds with $M = \text{Sc}$ and $P = \text{Sb}$ as well as $M = \text{Ti, Zr, Hf}$ and $P = \text{Sn}$, in their lowest-energy configurations, have a finite electronic energy gap (narrow-gap semiconductors). The next-higher-energy configurations are zero-gap semiconductors and the highest-energy configurations are always metallic. These changes in the electronic spectrum occur when the Ni d orbitals become less stable and produce greater hybridization near the Fermi level leading to an overlap of the conduction band with the valence band near the X point. The energy difference between this lowest-energy configuration and the configuration where Ni forms a part of the NaCl substructure range from 1.5–2.5 eV/unit cell, so are likely not to be seen experimentally.

An analysis of the energetics of antisite defects using different configurations of atoms within the supercell $(\text{NiMP})_4$ [specifically, $(\text{NiZrSn})_4$], shows that rearrangements of the MP NaCl substructure cost between 1.3–2.0 eV/fcc unit cell, while moving Ni atoms out of a fcc arrangement but keeping them within the octahedral pockets costs only about 0.5–0.8 eV/fcc unit cell. Since the Ni disorder is not seen while Zr/Sn antisite disorder is seen in NiZrSn after annealing,¹⁶ the Ni defects may be annealed out of the system while the ZrSn antisite defects, perhaps due to large energy barriers,

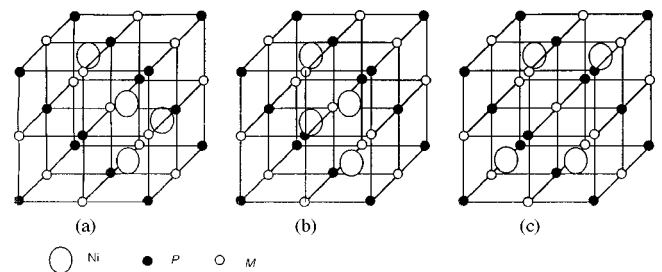


FIG. 8. Crystal structures of the $(\text{NiMP})_4$ supercell for rearrangements of the Ni sublattice.

may be quenched at low temperatures. Experimental measurement of the Ni disorder within the half-Heusler structure as a function of temperature is needed to better understand the energetics of Ni atoms within the octahedrally coordinated pockets.

The Zr/Sn antisite disorder in NiZrSn is believed to be due to the similarity of the atomic radii of Zr (0.160 nm) and Sn (0.158 nm) (Ref. 15) and has been suggested as a mechanism to reconcile the differences between the band gaps found experimentally to those found in the electronic structure calculations of the ordered NiZrSn.^{3,13,14} The effect of Ni disorder within the octahedrally coordinated pockets should also reduce the band gaps in the half-Heusler compounds. The experimental value of the band gap [~ 0.187 eV Ref. 15] for NiZrSn has been found much smaller than the value found in electronic structure calculations of the ordered compound [~ 0.51 eV Ref. 3]. The electronic structure calculations performed by OR in the virtual-crystal approximation found that the band gap in NiZrSn decreased with increasing Zr/Sn antisite disorder until going to zero for about 15% disorder.³ On the other hand, the atomic radii of Ti (0.147 nm) and Sn (0.158 nm) are quite different, so Ti/Sn antisite defects should be extremely rare in NiTiSn.¹⁵ How-

ever, the experimental value of the band gap in this compound [~ 0.120 eV (Ref. 15)] is also much smaller than that of the ordered NiTiSn obtained from electronic structure calculations [~ 0.51 eV (Ref. 3)]. Since one system displays antisite disorder in the NaCl sublattice while the other does not and yet the experimental and theoretical values of the band gap barely change, it seems unlikely that antisite disorder alone can explain the experimental and theoretical band-gap difference. Another mechanism seems necessary for explaining this difference. The fault may lie in the accuracy of the current electronic structure calculations (within LDA and GGA) to predict band gaps accurately. LDA (and GGA) is known to underestimate the band gaps in several systems.¹⁷ Improved methods beyond the LDA (and the GGA), such as the *GW* method,¹⁷ include correlation effects which have proven important in understanding the size of the gap in binary semiconductors and should be applied to the ternary systems studied in this paper.

ACKNOWLEDGMENT

This work was partly supported by DARPA Grant No. DAAG55-97-0184.

-
- ¹P. Larson, S. D. Mahanti, S. Sportouch, and M. G. Kanatzidis, *Phys. Rev. B* **59**, 15 660 (1999).
- ²S. D. Mahanti, P. Larson, D. Y. Chung, S. Sportouch, and M. G. Kanatzidis, *Mat. Res. Soc. Symp. Proc.* **545**, 23 (1999).
- ³S. Ogut and K. M. Rabe, *Phys. Rev. B* **51**, 10 443 (1995).
- ⁴K. E. H. M. Hannsen and P. E. Mijarends, *Phys. Rev. B* **34**, 5009 (1986).
- ⁵M. Springborg, B. Sang, and M.-L. Persson, *J. Phys.: Condens. Matter* **11**, 6169 (1999); J. Tobola, J. Pierre, S. Kaprzyk, R. V. Skolozdra, and M. A. Kouacou, *J. Magn. Magn. Mater.* **159**, 192 (1996); J. Tobola, J. Pierre, S. Kaprzyk, R. V. Skolozdra, and M. A. Kouacou, *J. Phys.: Condens. Matter* **10**, 1013 (1998).
- ⁶F. G. Aliev, *Physica B* **171**, 199 (1991); R. Keuntzler, R. Clad, G. Schmerber, and Y. Dossman, *J. Magn. Magn. Mater.* **104–107**, 1976 (1992); H. Hohl, A. P. Ramirez, K. Fess, Ch. Turner, Ch. Kloc, and E. Bucher, in *Thermoelectric Materials—New Directions and Approaches*, edited by T. M. Tritt, M. G. Kanatzidis, H. B. Lyon, Jr., and G. D. Mahan, *Mater. Res. Soc. Symp. Proc. No. 478* (Materials Research Society, Pittsburgh, 1997), p. 109; A. Slebarski, A. Jezierski, S. Lutkehoff, and M. Neumann, *Phys. Rev. B* **57**, 6408 (1998); C. Uher, J. Yang, S. Hu, D. T. Morelli, and G. P. Meisner, *ibid.* **59**, 8615 (1999); S. Sportouch, P. Larson, M. Bastea, P. Brazis, J. Ireland, C. R. Kannewurf, S. D. Mahanti, and M. G. Kanatzidis in *Thermoelectric Materials—the Next Generation Materials for Small-Scale Refrigeration and Power Generation Applications*, edited by T. M. Tritt, M. G. Kanatzidis, and H. B. Lyon, Jr., *MRS Symposia Proceedings No. 545* (Materials Research Society, Pittsburgh, 1999), p. 421.
- ⁷S. Ishida, T. Masaki, S. Fujii, and S. Asano, *Physica B* **237–238**, 363 (1997).
- ⁸D. Singh, *Plane Waves, Pseudopotentials, and the LAPW Method* (Kluwer Academic, Boston, 1994).
- ⁹P. Hohenberg and W. Kohn, *Phys. Rev.* **136**, B864 (1964); W. Kohn and L. Sham, *ibid.* **140**, A1133 (1965).
- ¹⁰J. P. Perdew and Y. Wang, *Phys. Rev. B* **45**, 13 244 (1992).
- ¹¹J. P. Perdew, K. Burke, and M. Ernzerhof, *Phys. Rev. Lett.* **77**, 3865 (1996).
- ¹²P. Blaha, K. Schwarz, and J. Luitz, *WIEN97* (Vienna University of Technology, Vienna, 1997).
- ¹³V. Ponnambalam, A. L. Pope, S. J. Poon, Y. Xia, S. Bhattacharya, and T. M. Tritt (unpublished).
- ¹⁴C. Uher, J. Yang, S. Hu, D. T. Morelli, and G. P. Meisner, *Phys. Rev. B* **59**, 8615 (1999).
- ¹⁵F. G. Aliev, A. I. Belogorkhov, N. B. Brandt, V. V. Kozyr'kov, R. V. Skolozdra, and Yu. V. Stadnyk, *Pis'ma Zh. Eksp. Teor. Fiz.* **47**, 151 (1987) [*JETP Lett.* **47**, 184 (1987)]; F. G. Aliev, V. V. Kozyrkov, V. V. Moshchalkov, R. V. Skolozdra, and K. Durczewski, *Z. Phys. B: Condens. Matter* **80**, 353 (1990); F. G. Aliev, *Physica B* **171**, 199 (1991).
- ¹⁶F. G. Aliev, N. B. Brandt, V. V. Kozyr'kov, V. V. Moshchalkov, R. V. Skolozdra, Yu. V. Stadnyk, and V. K. Pecharskii, *Pis'ma Zh. Eksp. Teor. Fiz.* **45**, 535 (1987) [*JETP Lett.* **45**, 684 (1987)]; F. G. Aliev, N. B. Brandt, V. V. Moshchalkov, V. V. Kozyrkov, R. V. Skolozdra, and A. I. Belogorkhov, *Z. Phys. B: Condens. Matter* **75**, 167 (1989).
- ¹⁷Wilfried G. Aulbur, Lars Jonsson, and John W. Willkins, in *Solid State Physics*, edited by H. Ehrenreich and F. Spaepen, Vol. 54 (Academic, Orlando, 2000), p. 1; F. Aryasetiawan and O. Gunnarson, *Rep. Prog. Phys.* **61**, 237 (1998); Xuejun Zhu and Steven G. Louie, *Phys. Rev. B* **43**, 14 142 (1991); S. B. Zhang, D. Thomanek, Marvin L. Cohen, Steven G. Louie, and Mark Hybertsen, *ibid.* **40**, 3162 (1989); Mark S. Hybertsen and Steven G. Louie, *ibid.* **34**, 5390 (1986).